Global trends in the interplane penetration depth of layered superconductors

S. V. Dordevic,* E. J. Singley, and D. N. Basov
Department of Physics, University of California, San Diego, La Jolla, California 92093

Seiki Komiya and Yoichi Ando
Central Research Institute of Electric Power Industry, Tokyo, Japan

E. Bucher†
Lucent Technologies, Murray Hill, New Jersey 07974

C. C. Homes and M. Strongin
Department of Physics, Brookhaven National Laboratory, Upton, New York 11973
(Received 4 September 2001; published 20 March 2002)

We report on generic trends in the behavior of the interlayer penetration depth λ_c of several different classes of quasi-two-dimensional superconductors including high-T_c cuprates, Sr_2RuO_4, transition-metal dichalcogenides and organic materials of the $(BEDT\text{-}TTF)_2X$ series. An analysis of these trends reveals two distinct patterns in the scaling between the values of λ_c and the magnitude of the *c*-axis dc conductivity σ_{dc}: one realized in the systems with a ground state formed from well-defined quasiparticles, and the other seen in systems in which the quasiparticles are not well defined. The latter pattern is found primarily in underdoped cuprates, and indicates a dramatic enhancement (a factor $\simeq 10^2$) of the energy scale Ω_C associated with the formation of the condensate compared to the data for conventional materials. We discuss the implication of these results on the understanding of superconductivity in high-T_c cuprates.

DOI: 10.1103/PhysRevB.65.134511 PACS number(s): 74.25.Gz, 78.20.−e

I. INTRODUCTION

The formation of a superconducting condensate in elemental metals and their alloys is well understood within the theory of Bardeen, Cooper, and Schrieffer (BCS) in terms of a pairing instability in the ensemble of Fermi-liquid (FL) quasiparticles. Applicability of the FL description to high-T_c cuprate superconductors is challenged by remarkable anomalies found in both the spin and charge responses of these compounds in the normal state.[1] Because quasiparticles are not well defined at $T>T_c$ in most cuprates it is natural to inquire into the distinguishing characteristics of a superconducting condensate which appears to be built from entirely different ''raw material.'' Infrared (IR) spectroscopy is perfectly suited for this task. Indeed, the analysis of the optical constants in the far-infrared unfolds the process of the formation of the condensate $\delta(0)$-peak in the dynamical conductivity,[2] and also gives insight into single-particle excitations in the system both above and below T_c.

In this paper we focus on the interplane properties of high-T_c superconductors. We will show that the distinctions in the behavior of the condensate in conventional superconductors and high-T_c cuprates are most radical in the case of the *c*-axis interplane response. The analysis of the generic trends seen in the behavior of the *c*-axis condensate (correlation between the penetration depth λ_c and the dc conductivity σ_{dc}) allows us to infer the energy scale Ω_C associated with the development of the superfluid in the cuprates. This energy scale may dramatically exceed the energy gap in systems lacking well-defined quasiparticles at $T>T_c$ (primarily in underdoped cuprates[3]). We discuss a connection between the magnitude of Ω_C and the nature of the normal-state response.

II. EXPERIMENTAL PROCEDURES

The response of the superconducting condensate can be investigated through IR experiments probing the complex conductivity $\sigma(\omega)=\sigma_1(\omega)+i\sigma_2(\omega)$ of a superconductor. At $T<T_c$ the real part of the conductivity can be written as

$$\sigma_1^{SC}(\omega)=\frac{\rho_s}{8}\delta(0)+\sigma_1^{reg}(\omega). \tag{1}$$

The $\delta(0)$-peak term represents the response of the condensate with the superfluid density $\rho_s=4\pi n_s e^2/m^*$ proportional to the concentration of superconducting carriers n_s, and inversely proportional to their effective mass m^*. The second term on the right-hand side of Eq. (1) is usually referred to as the regular component and represents the conductivity that is *not* due to the superconducting carriers. It may include conductivity due to unpaired carriers at $T<T_c$ at finite frequencies, phonons, interband transitions, magnons, etc. Commonly, the condensate stiffness is characterized through the penetration depth $\lambda=c/\sqrt{\rho_s}$, the notation we will use in this paper.

In order to discuss several techniques that can be exploited to determine the interlayer penetration depth of an anisotropic superconductor we turn to our data for $La_{1.83}Sr_{0.17}CuO_4$ (La214) with $T_c\simeq 36$ K (Fig. 1). Large single crystals were grown using the traveling-solvent floating-zone technique,[4] and were carefully annealed to remove excess oxygen. The crystallographic axes were deter-

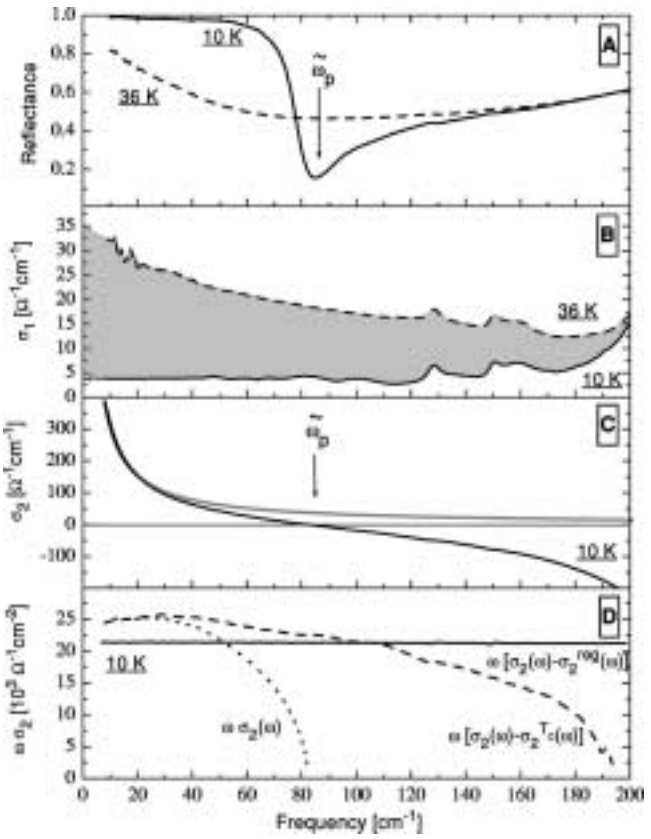

FIG. 1. Interlayer response of La214 single crystals with $T_c = 36$ K: reflectance $R(\omega)$ (panel A); real and imaginary parts of the conductivity (panels B and C) and the product $\sigma_2(\omega)\times\omega$ (panel D). The c-axis penetration depth can be determined from the IR data using several different techniques: from the position of the plasma minimum in $R(\omega)$, from integrating the difference between the $\sigma_1(\omega,T_c)$ and $\sigma_1(\omega,10K)$ [Eq. (2)], and from examining the frequency dependence of the $\sigma_2(\omega,10K)\times\omega$. The latter approach may underestimate the magnitude of λ_c because of the screening effects associated with the response of unpaired charge carriers at $T\ll T_c$. We employed Eqs. (3) and (4) to correct for this effect (solid line in panel D).

mined by Laue diffraction, and the samples were then cut into platelets with the ac planes parallel to the wide face. The error in the axes directions is less than 1°. Near-normal-incidence reflectance measurements were performed at UCSD in a frequency range between 10 and 48 000 cm^{-1} (1 meV–6 eV). The complex conductivity $\sigma(\omega)$ and complex dielectric function $\epsilon(\omega)=\epsilon_1(\omega)+i\epsilon_2(\omega_2)$ were inferred from $R(\omega)$ using Kramers-Kronig (KK) analysis. The low- and high-frequency extrapolations have negligible effects on the data in the measured frequency interval. Below we outline common analysis techniques used to determine the penetration depth from the results of IR studies.

(1) Raw *c*-axis reflectance of high-T_c superconductors at $T\ll T_c$ exhibits a sharp plasma edge. In the case of $La_{1.83}Sr_{0.17}CuO_4$ this feature is located at ~ 85 cm^{-1} (Fig. 1, panel A). This behavior is in contrast to the featureless normal-state reflectance. The position of the plasma edge is determined by the screened plasma frequency $\tilde{\omega}_p$, from which the penetration depth can be obtained as $c^2/\lambda^2=\tilde{\omega}_p^2\epsilon_\infty$ (Ref. 5). In the latter equation ϵ_∞ is the real part of the dielectric constant $\epsilon_1(\omega)$ at frequencies above the plasma edge. The numerical value of ϵ_∞ is somewhat ambiguous, and introduces an error in the result for λ_c. This technique was employed in Refs. 6–9.

(2) In a BCS superconductor the formation of the condensate is adequately described with the Ferrel-Glover-Tinkham (FGT) sum rule

$$\rho_s=\frac{c^2}{\lambda^2}=\int_{0+}^{\Omega_C}[\sigma_1^N(\omega)-\sigma_1^{reg}(\omega)]d\omega, \qquad (2)$$

where $\sigma_1^N(\omega)$ is the normal-state conductivity at T_c, and the upper integration limit Ω_C is of the order of the gap energy. The upper cutoff issue for cuprates will be discussed in detail below. According to this sum rule the area ''missing'' from the normal-state conductivity (shaded region in Fig. 1, panel B) is recovered under the $\delta(0)$ peak. This technique may somewhat underestimate the magnitude of λ_c because, at least in underdoped cuprates, the superfluid density is accumulated from a broad energy region significantly exceeding the gap energy.[2,8,10,11] This method was used for an analysis of the penetration depth in Refs. 12–14.

(3) Finally, the most commonly used method of extracting λ_c is based on the examination of the imaginary part of the complex optical conductivity. By KK transformation, the δ peak at $\omega=0$ in the real part of the optical conductivity implies that the imaginary part has the form $\sigma_2(\omega)=c^2/(4\pi\omega\lambda^2)$. Therefore, the magnitude of λ_c can be estimated from $\omega\times\sigma_2(\omega)$ in the limit of $\omega\to 0$ (the gray line in panel C of Fig. 1 or the dotted line in panel D) (Refs. 2,6,8,10,11 and 15–18).

While method 3 is very well suited to quantify the magnitude of the penetration depth, this technique also may introduce systematic errors. Strictly speaking, the relation $\sigma_2(\omega)=c^2/(4\pi\omega\lambda^2)$ is valid only if $\sigma_1^{reg}(\omega)=0$. Typically, this is not the case in high-T_c superconductors, which all show residual absorption in the far-IR conductivity. This absorption may be (in part) connected with *d*-wave symmetry of the order parameter in cuprates[1] leading to gapless behavior at any finite temperature. Data displayed in Fig. 1, panel B, clearly shows a nonvanishing IR conductivity down to the lowest T and ω. A finite regular contribution to $\sigma_1(\omega)$ implies a finite contribution to $\sigma_2(\omega)$. Owing to this contribution the spectra of $\sigma_2(\omega)$ acquire a complicated frequency dependence that may significantly differ from the $1/\omega$ form (Fig. 1, panels C and D). Moreover, the magnitude of the penetration depth extracted from such a spectrum is likely to be underestimated, even if the product $\sigma_2(\omega)\times\omega$ is taken at the lowest experimentally accessible frequencies.

Systematic errors in the magnitude of λ connected with $\sigma_1^{reg}(\omega)>0$ can be eliminated using the following procedure. The intrinsic value of the penetration depth can still be determined from $\sigma_2(\omega)$, if the imaginary part of the conductivity is corrected by $\sigma_2^{reg}(\omega)$ characterizing all screening effects that are not due to superconducting carriers at $T<T_c$:

$$\sigma_2(\omega)-\sigma_2^{reg}(\omega)=\frac{c^2}{4\pi\omega\lambda^2}. \quad (3)$$

To determine $\sigma_2^{reg}(\omega)$ we employ a KK-like transformation:

$$\sigma_2^{reg}(\omega)=-\frac{2\omega}{\pi}\int_{0^+}^{\infty}\frac{\sigma_1^{reg}(\omega')}{\omega'^2-\omega^2}d\omega'. \quad (4)$$

The result of the application of the correction procedure for the imaginary part of the conductivity is presented in Fig. 1, panel D. It appears that after subtraction of $\sigma_2^{reg}(\omega)$, the remaining contribution to the conductivity reveals a $1/\omega$ behavior over an extended frequency region, supporting the soundness of the procedure proposed here. We emphasize again that *no other* correction procedure besides that described by Eqs. (3) and (4) has been used. In the case of $La_{1.83}Sr_{0.17}CuO_4$, the latter procedure leads only to a minor correction of the absolute value of λ_c ($\sim$18%). That is because the absolute value of $\sigma_1^{reg}(\omega)$ is relatively small and is constant throughout far-IR (Fig. 1, panel B). However, such a correction can be much more significant for overdoped samples, which often show stronger Drude-like contributions in $\sigma_1^{reg}(\omega)$ spectra. Figure 1, panel D also shows a frequently used approximation to the method we have just outlined: instead of subtracting $\sigma_2^{reg}(\omega)$, one subtracts $\sigma_2(\omega,T_c)$ from $\sigma_2(\omega,T\ll T_c)$. The resulting curve looks somewhat better than the uncorrected one, but still yields an enhanced value of $\omega\times\sigma_2(\omega)$ in the limit of $\omega\rightarrow 0$.

III. UNIVERSAL *c*-AXIS PLOT

The *c*-axis penetration depth in a layered superconductor can be determined from IR experiments,[2,6–18] as described in Sec. II. In addition, several other experimental techniques, including magnetization measurements,[19–26] microwave absorption,[27–33] and vortex imaging[34,35] can be used to determine the magnitude of λ_c. Regardless of the method employed, the interlayer penetration depth in several families of cuprates reveals a universal scaling behavior with the magnitude of $\sigma_{dc}(T=T_c)$ (Fig. 2) (Ref. 15): the absolute value of λ_c is systematically suppressed with the increase of the normal state conductivity.[36] The scaling is obeyed primarily in underdoped cuprates (blue symbols in Fig. 2) . The deviations from the scaling are also systematic, and are most prominent in overdoped phases (red symbols in Fig. 2). Such deviations are a direct consequence of a well-established fact: on the overdoped side of the phase diagram σ_{dc} increases, whereas λ_c is either unchanged or may show a minor increase.[10,16,37]

We find a similar scaling pattern between λ_c and σ_{dc} in other classes of layered superconductors, including organic materials, transition metal dichalcogenides and Sr_2RuO_4 (Fig. 2). While the noncuprate data set is not nearly as dense, the key trend is analogous to the one found for cuprates. The slope of the $\lambda_c-\sigma_{dc}$ dependence is also close for both cuprates and noncuprate materials. The principal difference is that the cuprates universal line is shifted down by approximately one order of magnitude in λ_c. The latter result shows that the superfluid density ($\propto 1/\lambda^2$) is significantly enhanced in underdoped cuprates compared to noncuprate materials with the same dc conductivity.

Possible origins of the $\lambda_c-\sigma_{dc}$ correlation were recently discussed in the literature.[38] A plausible qualitative account of this effect can be based on the FGT sum rule [Eq. (2)]. For a dirty limit superconductor $\sigma_1^N(\omega)\approx\sigma_{dc}$, and Eq. (2) can be approximated as:

$$\rho_s=\frac{c^2}{\lambda^2}\approx 2\Delta\sigma_{dc}. \quad (5)$$

Such an approximation is possible because within the BCS model the energy scale Ω_C from which the condensate is collected is of the order of magnitude of the gap: $\Omega_C\simeq 2\Delta\simeq(3-5)kT_c$. A connection between $1/\lambda^2$, σ_{dc} and 2Δ is illustrated in the inset of Fig. 2. In the dirty limit the magnitude of σ_{dc} sets the amount of spectral weight available in the normal-state conductivity, whereas the magnitude of $\Omega_C\simeq 2\Delta$ defines the fraction of this weight which is transferred into condensate at $T<T_c$. Therefore, the magnitude of λ_c can be expected to decrease systematically with the enhancement of the dc conductivity, in accord with the FGT sum rule. Notably, an approximate form [Eq. (5)] yields the $\lambda_c-\sigma_{dc}$ scaling with the power law $\alpha=1/2$ which is close to $\alpha=0.59$ seen in Fig. 2.

The strong condensate density in the cuprates can be understood in terms of the dramatic enhancement of the energy scale Ω_C over the magnitude of the energy gap. This can be seen through a comparison of the universal scaling patterns observed for cuprates and of a similar pattern detected for noncuprate superconductors. The energy scale associated with the condensate formation for materials on the upper line, which for most conventional materials in Fig. 2 is close to estimates of the gap, is of the order of 1–3 meV. In Sr_2RuO_4, for example, $2\Delta=2.2$ meV, based on Andreev reflection measurements.[39] If Eq. (5), in the form $\rho_s=c^2/\lambda^2\approx\Omega_C\sigma_{dc}$ appropriate for cuprates, is employed to describe the difference between the upper and lower lines in Fig. 2, then one can conclude that the corresponding scale for underdoped cuprates is $\sim$100 times greater, i.e., of the order 0.1–0.3 eV. This assessment of Ω_C is supported by the explicit sum-rule analysis for several cuprates,[2,11] and also makes Ω_C the largest energy scale in the problem of cuprate superconductivity.[40]

Data points in Fig. 2 for overdoped materials support the notion that the $\lambda_c-\sigma_{dc}$ plot provides a means to learn about the energy scale associated with the condensate formation. Deflection of the overdoped cuprates from the universal line implies that Ω_C is gradually suppressed with increased carrier density. This trend is common for $Tl_2Ba_2CuO_{6+\delta}$ (Tl2201), La214 and $YBa_2Cu_3O_{7-\delta}$ (YBCO) materials (see Fig. 2). Integration of the conductivity for all these overdoped materials shows that the FGT sum rule is exhausted at energies as low as 0.08 eV (Refs. 10 and 11).

In BCS superconductors Ω_C is related to 2Δ, and therefore to T_c. In cuprates we find no obvious connection between the broad energy scale Ω_C and the critical temperature

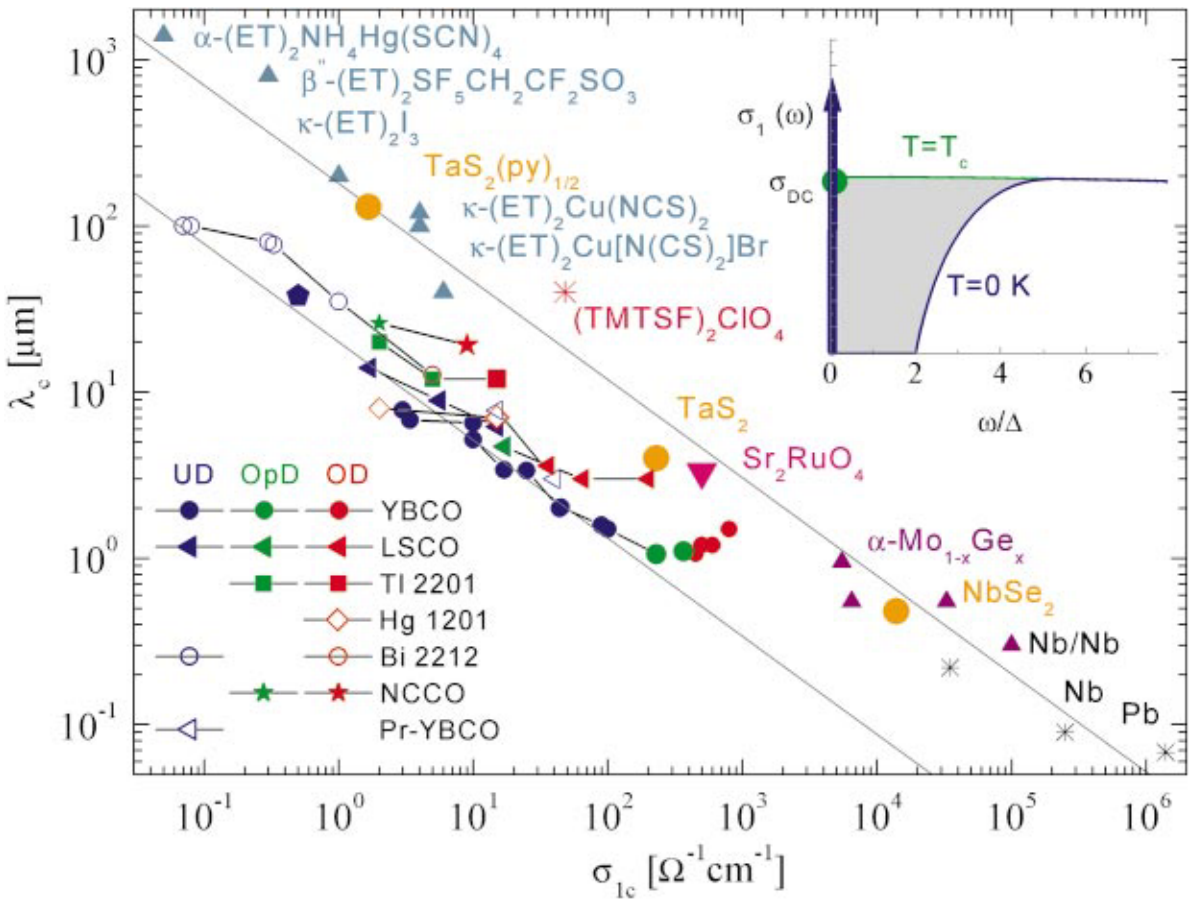

FIG. 2. (Color) The *c*-axis penetration depth $\lambda_c(T \cong 0K)$ as a function of the *c*-axis dc conductivity $\sigma_{1c}(T_c)$. We find two distinct patterns of $\lambda_c - \sigma_{dc}$ scaling. Cuprate superconductors exhibit much shorter penetration depths than noncuprate materials with the same $\sigma_{dc}(T_c)$. This result implies a dramatic enhancement of the energy scale Ω_C from which the condensate is collected, as described in the text. The superconducting transition temperature T_c has not been found to be relevant to the $\lambda_c - \sigma_{dc}$ scaling. Data points: YBCO (Refs. 6,15, and 17), overdoped YBCO (Refs. 12–15), La214 (Refs. 6,16,18, and 33), $HgBa_2Cu_2O_4$ (Refs. 34 and 59), Tl2201 (Refs. 2,10 and 35), $Bi_2Sr_2CaCu_2O_8$ (Refs. 7 and 23), and $Nd_{2-x}Ce_xCuO_4$ (Refs. 8 and 27). Blue points, underdoped (UD); green points, optimally doped (OpD); red points overdoped (OD). Transition-metal dichalcogenides (Refs. 19–21,47 and 60–62), $(ET)_2X$ compounds (Refs. 22,24,25,28–30, and 63–65), $(TMTSF)_2ClO_4$ (Refs. 66 and 67), Sr_2RuO_4 (Refs. 26 and 68), niobium (Refs. 31 and 32), lead (Ref. 32), niobium Josephson junctions (Ref. 69), and $\alpha Mo_{1-x}Ge_x$ (Ref. 70). Inset: in a conventional dirty limit superconductor the spectral weight of the superconducting condensate (given by $1/\lambda^2$) is collected primarily from the energy-gap region (gray). The total normal weight is preset by magnitude of σ_{dc}, whereas the product of $2\Delta \times \sigma_{DC}$ quantifies the fraction of the weight that condenses.

T_c. While scaling of λ_c by the magnitude of T_c does reduce the "scattering" of the data points,[33,38] the two distinct $\lambda_c - \sigma_{dc}$ patterns persist even if such scaling is implemented. Similarly, the difference between the two lines in Fig. 2 cannot be accounted for by differences in T_c. In particular, the critical temperature of strongly underdoped La214 materials is nearly the same as that of the several ET compounds ($\simeq$12–15 K). Nevertheless, the penetration depth is dramatically enhanced in the latter systems.

IV. IN-PLANE QUASIPARTICLES AND INTERPLANE TRANSPORT

A quick inspection of the materials in Fig. 2 suggests that a smaller condensate scale (top line) is observed in systems in which superconductivity emerges out of a normal state with well-defined quasiparticles, whereas the enhanced value of Ω_C is found in underdoped cuprates for which the quasiparticle concept may not apply (bottom line). The experiments which in our opinion are most relevant to this classification include quantum oscillations of the low-*T* interlayer resistivity (and of other quantities) in high magnetic fields.[41] Quantum oscillations can be viewed as a direct testimony of long-lived quasiparticles capable of propagating coherently between the layers. Indeed, quantum oscillations were observed in two-dimensional organic superconductors,[41,42] 2H-$NbSe_2$ (Ref. 43) and Sr_2RuO_4 (Ref. 44). Conversely, quantum oscillations have never been reported for underdoped cuprates. The lack of coherence in the *c*-axis transport in these materials indicates that the ground state of cuprates may be fundamentally different.

Signatures of coherent and incoherent behavior can also be recognized in the spectra of the *c*-axis conductivity. A hallmark of a coherent response is the Drude peak seen in

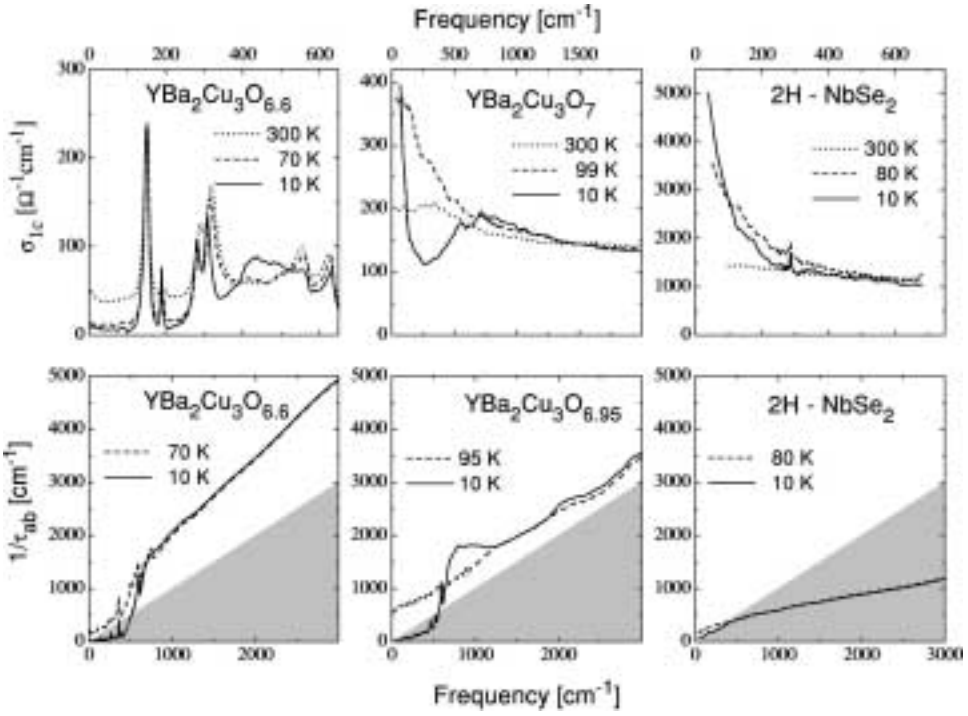

FIG. 3. Examples of the interplane transport for layered superconductors. Top panels show the out-of-plane optical conductivity $\sigma_c(\omega)$, and the bottom panels the corresponding in-plane scattering rate $1/\tau_{ab}(\omega)$. The observation of the Drude-like feature in the interplane optical conductivity of the dichalcogenide 2H-$NbSe_2$ (top right panel) is consistent with magnetoresistance measurements that reveal evidence of well-behaved quasiparticles. In contrast the conductivity of underdoped $YBa_2Cu_3O_{6.6}$ material (top, left panel) gives no signs of coherent response. Overdoped cuprates show the emergence of a Drude-like feature (top, middle panel) and also occupy an intermediate position between the two lines in Fig. 2. Experimental data: $YBa_2Cu_3O_{6.6}$ (Refs. 52 and 71), $YBa_2Cu_3O_7$ (Refs. 13 and 14), $YBa_2Cu_3O_{6.95}$ (Ref. 52), and 2H-$NbSe_2$ (Ref. 46).

$\sigma_1(\omega)$ of metals. Notably, a similar feature has never been found in the *c*-axis response of underdoped compounds (forming the lower line in Fig. 2). The electronic contribution to $\sigma_1(\omega)$ in these materials is usually structureless which is commonly associated with the incoherent (diffusive) motion of charge carriers across the planes. Conversely, many materials that belong to the upper line in Fig. 2 demonstrate a familiar Drude-like behavior. This kind of behavior was found in Sr_2RuO_4 (Ref. 45) and is also shown in our data[46] for the interplane response of 2H-$NbSe_2$ (Fig. 3, top right panel). In both cases, the width of the peak decreases at low temperatures, which is characteristic of the response of ordinary metals.[47] As for the over-doped cuprates (located in a cross-over region between the two lines in Fig. 2) their conductivity is indicative of the formation of the Drude-like peak [see, for example, $\sigma_c(\omega)$ for $YBa_2Cu_3O_7$; Fig. 3, top middle panel], which is becoming more pronounced with increased carrier density.[48]

Analysis of the anisotropic carrier dynamics in several layered superconductors indicates that the degree of coherence in the interplane transport may be related to the strength of inelastic scattering within the conducting planes. The bottom panels in Fig. 3 show the in-plane scattering rate (inverse lifetime) $1/\tau_{ab}(\omega)$ (Ref. 49) for the layered compounds corresponding to the top three panels.[50] In all these systems $1/\tau_{ab}(\omega) \propto \omega$ over an extended frequency interval (up to 3000 cm^{-1})[51]. An important feature of the data displayed in Fig. 3 is that as doping is increased from underdoped $YBa_2Cu_3O_{6.6}$ to optimally doped $YBa_2Cu_3O_{6.95}$ the absolute values of $1/\tau_{ab}(\omega)$ decrease. A similar trend is observed in other cuprate families.[52–55] The shaded regions in Fig. 3 represent a Landau-Fermi-liquid (LFL) regime, where the quasiparticles are well defined, i.e., the magnitude of the scattering rate is smaller than the energy $[1/\tau(\omega) \leqslant \omega]$. In 2H-$NbSe_2$ $1/\tau_{ab}(\omega, 10K)$ is in the LFL regime over the entire frequency interval displayed in Fig. 3. However, this is not the case for the two cuprates discussed. We believe that these differences in absolute values may have a profound effect on the *interplane* transport. In 2H-$NbSe_2$, where the in-plane quasiparticles are well defined, the interplane transport is also coherent, and is characterized by a narrow Drude-like mode whose width decreases with temperature (Fig. 3, top right panel). On the other hand, in $YBa_2Cu_3O_{6.6}$, which lacks well-defined quasiparticles, the interplane transport is incoherent, with $\sigma_1(\omega)$ being dominated by optical phonons (Fig. 3, top right panel). As for the over-doped $YBa_2Cu_3O_7$ (Fig. 3, bottom middle panel) the optical conductivity of this compound is in between these two opposite limits. Figure 3 therefore supports the notion that long-lived in-plane quasiparticles may be one of the necessary prerequisites for coherent out-of-plane transport.

V. GLOBAL TRENDS IN LAYERED SUPERCONDUCTORS

To summarize the experimental results reported in this work, we wish to stress the following points: (i) two distinct

patterns in $\lambda_c - \sigma_{dc}$ correlation (Fig. 2) are indicative of a dramatic difference ($\simeq 10^2$) in the energy scale Ω_C from which the interlayer condensate is collected; (ii) the pattern with the typical energy scale of the order of meV is realized in the materials with the coherent transport between the planes, whereas the one with a strongly enhanced value of Ω_C is found in underdoped cuprate superconductors with an incoherent response; (iii) overdoped cuprates reveal a crossover between the two behaviors; and (iv) the coherence in the interlayer transport correlates with the strength of inelastic scattering within the conducting planes (Fig. 3). These results allow us to draw several conclusions regarding features of the superconducting condensate in different layered systems.

(i) The symmetry of the order parameter seems to be unrelated to trends seen in the c-axis condensate response. Indeed, the upper line in Fig. 2 is formed by *s*-wave transition-metal dichalcogenides, *p*-wave Sr_2RuO_4, and organic materials for which both *s*- and *d*-wave states have been proposed,[41] while *d*-wave high-T_c materials form the lower line and the crossover region between the lines.

(ii) The electrodynamics of the systems on the top line at $T \ll T_c$ is determined by the magnitude of the gap (and hence by T_c), in general agreement with BCS theory. It is therefore hardly surprising that the trend initiated by two-dimnesional superconductors is also followed in one-dimensional organic conductors, as well as by more conventional systems such as Nb Josephson junctions, bulk Nb and Pb or amorphous $\alpha Mo_{1-x}Ge_x$ (see Fig. 2).

(iii) While the pseudogap state has been shown to be responsible for the anomalous superfluid response of the underdoped cuprates,[2,11] the characteristic pseudogap temperature $T^* = 90-350$ K is still much lower than our estimate of Ω_C for these materials (0.1–0.3 eV, i.e., 1000–3000 K).

(iv) Unlike BCS superconductors, where T_c is determined by 2Δ and therefore by Ω_C, the critical temperature T_c in cuprates correlates with neither 2Δ nor Ω_C.

In conclusion, analyzing a large amount of experimental data, we found two distinctly different patterns in $\lambda_c - \sigma_{dc}$ scaling in layered superconductors. Based on the universal *c*-axis plot, we inferred a broad energy scale Ω_c relevant for pair formation in underdoped cuprates. This result is consistent with the idea that the superconducting transition in the cuprates is driven by a lowering of the electronic kinetic energy.[72] We argue that the appearance of such an energy scale is fundamentally related to the incoherent *c*-axis transport, which, on the other hand, may be related to poorly defined in-plane quasiparticles. A quantitative account of the distinct energy scales associated with the condensate is a challenge for models attempting to solve the puzzle of cuprate superconductivity.

ACKNOWLEDGMENTS

The research at UCSD was supported by the NSF, the U.S. DOE, and the Research Corporation. The work at Brookhaven National Laboratory was supported, in part, by the U.S. Department of Energy, Division of Materials Science, under Contract No. DE-AC02-98CH10886.

*Electronic address: sasa@physics.ucsd.edu

†Also at Fakultät für Physik, Universität Konstanz, D-78457 Konstanz, Germany.

[1] J. Orenstein and A. J. Millis, Science **288**, 468 (2000).

[2] D. N. Basov, S. I. Woods, A. S. Katz, E. J. Singley, R. C. Dynes, M. Xu, D. G. Hinks, C. C. Homes, and M. Strongin, Science **283**, 49 (1999).

[3] Underdoped cuprates are compounds whose carrier doping level is smaller than optimal (the one with the highest T_c).

[4] Y. Ando, A. N. Lavrov, S. Komiya, K. Segawa, and X. F. Sun, Phys. Rev. Lett. **87**, 017 001 (2001).

[5] T. Timusk and D. B. Tunner, in *Physical Properties of High Temperature Superconductors I*, edited by D. M. Ginsberg (World Scientific, Singapore, 1989).

[6] S. Uchida and K. Tamasaku, Physica C **293**, 1 (1997).

[7] T. Motohashi, J. Shimoyama, K. Kitazawa, K. Kishio, K. M. Kojima, S. Uchida, and S. Tajima, Phys. Rev. B **61**, 9269 (2000).

[8] E. J. Singley, D. N. Basov, K. Kurahashi, T. Uefuji, and K. Yamada, Phys. Rev. B **64**, 224503 (2001).

[9] A. A. Tsvetkov, D. van der Marel, K. A. Moler, J. R. Kirtley, J. L. de Boer, A. Meetsma, Z. F. Ren, N. Koleshnikov, D. Dulic, A. Damascelli, M. Gruninger, J. Schutzmann, J. W. van der Eb, H. S. Somal, and J. H. Wang, Nature (London) **395**, 360 (1998).

[10] A. S. Katz, S. I. Woods, E. J. Singley, T. W. Li, M. Xu, D. G. Hinks, R. C. Dynes, and D. N. Basov, Phys. Rev. B **61**, 5930 (2000).

[11] D. N. Basov, C. C. Homes, E. J. Singley, M. Strongin, T. Timusk, G. Blumberg, and D. van der Marel, Phys. Rev. B **63**, 134514 (2001).

[12] C. Bernhard, D. Munzar, A. Wittlin, W. Konig, A. Golnik, C. T. Lin, M. Klaser, T. Wolf, G. Muller-Vogt, and M. Cardona, Phys. Rev. B **59**, 6631 (1999).

[13] J. Schutzmann, S. Tajima, S. Miyamoto, and S. Tanaka, Phys. Rev. Lett. **73**, 174 (1994).

[14] S. Tajima, J. Schutzmann, S. Miyamoto, I. Terasaki, Y. Sato, and R. Hauff, Phys. Rev. B **55**, 6051 (1997).

[15] D. N. Basov, T. Timusk, B. Dabrowski, and J. D. Jorgensen, Phys. Rev. B **50**, 3511 (1994).

[16] S. Uchida, K. Tamasaku, and S. Tajima, Phys. Rev. B **53**, 14 558 (1996).

[17] C. C. Homes, T. Timusk, D. A. Bonn, R. Liang, and W. N. Hardy, Physica C **254**, 265 (1995).

[18] D. N. Basov, H. A. Mook, B. Dabrowski, and T. Timusk, Phys. Rev. B **52**, 13 141 (1995).

[19] P. de Trey, S. Gygax, and J.-P. Jan, J. Low Temp. Phys. **11**, 421 (1973).

[20] D. J. Huntley and R. F. Frindt, in *Physics and Chemistry of Materials With Layered Structures* (Reidel, Dordrecht, 1976).

[21] K. Onabe, M. Naito, and S. Tanaka, J. Phys. Soc. Jpn. **45**, 50 (1978).

[22] A. Carrington, I. J. Bonalde, R. Prozorov, R. W. Giannetta, A. M. Kini, J. Schlueter, H. H. Wang, U. Geiser, and J. M. Williams, Phys. Rev. Lett. **83**, 4172 (1999).

[23] J. R. Cooper, L. Forro, and B. Keszei, Nature (London) **343**, 444 (1990).

[24] H. Taniguchi, H. Sato, Y. Nakazawa, and K. Kanoda, Phys. Rev. B **53**, 8879 (1996).

[25] S. Wanka, D. Beckmann, J. Wosnitza, E. Balthes, D. Schweitzer, W. Strunz, and H. J. Keller, Phys. Rev. B **53**, 9301 (1996).

[26] K. Yoshida, Y. Maeno, S. Nishizaki, and T. Fujita, Physica C **263**, 519 (1996).

[27] A. Pimenov, A. V. Pronin, A. Loidl, U. Michelucci, A. P. Kampf, S. I. Krasnosvobodtsev, V. S. Nozdrin, and D. Rainer, Phys. Rev. B **62**, 9822 (2000).

[28] T. Shibauchi, M. Sato, A. Mashio, T. Tamegai, H. Mori, S. Tajima, and S. Tanaka, Phys. Rev. B **55**, 11 977 (1997).

[29] M. Dressel, O. Klein, G. Gruner, K. D. Carlson, H. H. Wang, and J. M. Williams, Phys. Rev. B **50**, 13 603 (1994).

[30] R. Prozorov, R. W. Giannetta, J. Schlueter, A. M. Kini, J. Mohtasham, R. W. Winter, and G. L. Gard, Phys. Rev. B **63**, 052506 (2001).

[31] A. V. Pronin, M. Dressel, A. Pimenov, A. Loidl, I. V. Roshchin, and L. H. Greene, Phys. Rev. B **57**, 14 416 (1998).

[32] O. Klein, E. J. Nicol, K. Holczer, and G. Gruner, Phys. Rev. B **50**, 6307 (1994).

[33] T. Shibauchi, H. Kitano, K. Uchinokura, A. Maeda, T. Kimura, and K. Kishio, Phys. Rev. Lett. **72**, 2263 (1994).

[34] J. R. Kirtley, K. A. Moler, G. Villard, and A. Maignan, Phys. Rev. Lett. **81**, 2140 (1998).

[35] K. A. Moler, J. R. Kirtley, D. G. Hinks, T. W. Li, and M. Xu, Science **279**, 1193 (1998).

[36] Whenever available λ_c and σ_{dc} values obtained from IR spectroscopy were used, and as shown here the errors of such measurements do not exceed 15–20 %. This error includes the error introduced by the uncertainty of reflectance measurements, which is typically around 1%. When IR spectroscopic data were not available (particularly for the compounds on the top line in Fig. 2), we used the results from other experimental techniques mentioned in the text. Typical errors, as reported in the original publications, are $<10\%$ for microwave absorption (Ref. 31), $\sim 20\%$ for magnetization (Ref. 22), $<30\%$ for vortex imaging (Ref. 35), and $\sim 5\%$ for resistivity (i.e., $1/\sigma_{dc}$) measurements. When the results from different measurements on the same compound differed substantially, for example λ_c values for κ(BEDT-TTF)$_2$Cu[N(CS)$_2$]Br (Refs. 22 and 29), they were both shown in Fig. 2. We emphasize that errors as high as 20% cannot in any significant way change a plot that spans several orders of magnitude.

[37] C. Panagopoulos, J. R. Cooper, T. Xiang, Y. S. Wang, and C. W. Chu, Phys. Rev. B **61**, 3808 (2000).

[38] W. Kim and J. P. Carbotte, Phys. Rev. B **61**, 11 886 (2000); Y. Ohashi, J. Phys. Soc. Jpn. **69**, 659 (2000); P. J. Hirschfeld, S. M. Quinlan, and D. J. Scalapino, Phys. Rev. B **55**, 12 742 (1997); S. Chakravarty, Hae-Young Kee, and E. Abrahams, Phys. Rev. Lett. **82**, 2366 (1999).

[39] F. Laube, G. Goll, H. v. Lohneysen, M. Fogelstrom, and F. Lichtenberg, Phys. Rev. Lett. **84**, 1595 (2000).

[40] The sum-rule arguments discussed in this section may help one understand the rationale behind the universal $\lambda_c - \sigma_{dc}$ scaling in underdoped cuprates. That is, despite the fact that the superconducting energy gap is not well defined in the interlayer conductivity of these materials. The gapless response of cuprates is exemplified in Fig. 1 panel B and the top-left panel of Fig. 3 displaying $\sigma_1(\omega)$ data for $YBa_2Cu_3O_{6.6}$ with $T_c \simeq 60$ K. The normal-state conductivity is suppressed as the sample is cooled down to T_c, with a transfer of spectral weight to higher energies. Below T_c, one does not find any radical changes in the $\sigma_1(\omega)$ spectra. Most importantly, this system, along with all other underdoped compounds, shows significant absorption in the superconducting state so that $\sigma_1^{reg} > 0$. Therefore, in cuprates only a *small fraction* of the far-infrared spectral weight contributes to the condensate. The latter result is in apparent conflict with the assumption $\sigma_1^{reg}(\omega < 2\Delta) \simeq 0$, which allows one to reduce Eq. (2) to the approximate form given by Eq. (5). However, the strong condensate density seen in the cuprates located on the universal line can be understood in terms of a dramatic enhancement of the energy scale Ω_C over the magnitude of the energy gap. This latter conclusion also follows from the explicit sum-rule analysis for samples of underdoped $La_{2-x}Sr_xCuO_4$ (La214), $YBa_2Cu_3O_{7-\delta}$ (YBCO), and $Tl_2Ba_2CuO_{6+\delta}$ (Tl2201) materials, suggesting that Ω_C in these compounds exceeds 0.1-0.2 eV (Ref. 2,10,11).

[41] J. Wosnitza, *Fermi Surfaces of Low-Dimensional Organic Metals and Superconductors* (Springer, Berlin, 1996).

[42] J. Singleton, P. A. Goddard, A. Ardavan, N. Harrison, S. J. Blundell, J. A. Schlueter, and A. M. Kini, Phys. Rev. Lett. **87**, 117001 (2001).

[43] R. Corcoran, P. Meeson, Y. Onuki, P.-A. Probst, M. Springford, K. Takita, H. Harima, G. Y. Guo, and B. L. Gyorffy, J. Phys.: Condens. Matter **6**, 4479 (1994).

[44] C. Bergemann, S. R. Julian, A. P. Mackenzie, S. NishiZaki, and Y. Maeno, Phys. Rev. Lett. **84**, 2662 (2000).

[45] T. Katsufuji, M. Kasai, and Y. Tokura, Phys. Rev. Lett. **76**, 126 (1996).

[46] S. V. Dordevic, D. N. Basov, R. C. Dynes, and E. Bucher, Phys. Rev. B **64**, 161103 (2001).

[47] Earlier measurements of the *c*-axis infrared absorption proved the applicability of conventional BCS electrodynamics to the 2H-$NbSe_2$ data. See R. J. Kennedy and B. P. Clayman, Can. J. Phys. **62**, 776 (1984).

[48] We emphasize that the observation of a Drude-like mode in the optical spectra is consistent with, but not a definite proof of, coherent interlayer transport. Similarly, the absence of a zero-energy mode does not necessarily imply incoherent transport. Recent c-axis IR experiments on two-dimensional (2D) organic superconductors (Ref. 56) seemed to indicate the absence of a Drude-like mode in these compounds. However, high-magnetic-field measurements (Refs. 41 and 42) undoubtedly show the existence of a 3D Fermi surface, i.e., well-defined quasiparticles that can propagate coherently between the layers.

[49] The scattering rate can be calculated from IR data as

$$\frac{1}{\tau_{ab}(\omega)} = \frac{\omega_p^2}{4\pi} \frac{\sigma_1(\omega)}{\sigma_1^2(\omega) + \sigma_2^2(\omega)},$$

where ω_p is the plasma frequency, and can be obtained from the integration of the optical conductivity $\sigma_1(\omega)$ up to the frequency corresponding to the onset of interband absorption. See Ref. 55 for a review.

[50] Because in-plane measurements of $YBa_2Cu_3O_7$ are not available, we have used $1/\tau_{ab}(\omega)$ data for $YBa_2Cu_3O_{6.95}$. We believe that

this does not affect the conclusions of the paper in any significant way.

[51] Many other 2D conductors also show a linear frequency dependence of the in-plane scattering rate. In particular, this behavior was reported for graphite (Ref. 57), 2H-$TaSe_2$, and other transition metal dichalcogenides (Ref. 58) and a variety of cuprates (Refs. 52–55).

[52] D. N. Basov, R. Liang, B. Dabrowski, D. A. Bonn, W. N. Hardy, and T. Timusk, Phys. Rev. Lett. **77**, 4090 (1996).

[53] A. V. Puchkov, P. Fournier, D. N. Basov, T. Timusk, A. Kapitulnik, and N. N. Kolesnikov, Phys. Rev. Lett. **77**, 3212 (1996).

[54] L. D. Rotter, Z. Schlesinger, R. T. Collins, F. Holtzberg, C. Field, U. W. Welp, G. W. Crabtree, J. Z. Liu, Y. Fang, K. G. Vandervoort, and S. Fleshler, Phys. Rev. Lett. **67**, 2741 (1991).

[55] A. V. Puchkov, D. N. Basov, and T. Timusk, J. Phys.: Condens. Matter **8**, 10 049 (1996).

[56] J. J. McGuire, T. Room, A. Pronin, T. Timusk, J. A. Schlueter, M. E. Kelly, and A. M. Kini, Phys. Rev. B **64**, 094503 (2001).

[57] S. Xu, J. Cao, C. C. Miller, D. A. Mantell, R. J. D. Miller, and Y. Gao, Phys. Rev. Lett. **76**, 483 (1996).

[58] T. Valla, A. V. Fedorov, P. D. Johnson, J. Xue, K. E. Smith, and F. J. DiSalvo, Phys. Rev. Lett. **85**, 4759 (2000); V. Vescoli, L. Degiorgi, H. Berger, and L. Forro, *ibid.* **81**, 453 (1998).

[59] E. J. Singley and D. N. Basov (private communication).

[60] P. Garoche, J. J. Veyssie, P. Manuel, and P. Molinie, Solid State Commun. **19**, 455 (1976).

[61] J. J. Finley and B. S. Deaver, Solid State Commun. **36**, 493 (1980).

[62] A. H. Thompson, F. R. Gamble, and R. F. Koehler, Phys. Rev. B **5**, 2811 (1972).

[63] X. Su, F. Zuo, J. A. Schlueter, A. M. Kini, and Jack M. Williams, Phys. Rev. B **58**, 2944 (1998).

[64] K. Kajita, Y. Nishio, S. Moriyama, W. Sasaki, R. Kato, H. Kobayashi, and A. Kobayashi, Solid State Commun. **64**, 1279 (1987).

[65] X. Su, F. Zuo, J. A. Schlueter, J. M. Williams, P. G. Nixon, R. W. Winter, and G. L. Gard, Phys. Rev. B **59**, 4376 (1999).

[66] H. Schwenk, K. Andres, F. Wudl, and E. Aharon-Shalom, Solid State Commun. **45**, 767 (1983).

[67] K. Murata, H. Anzai, G. Saito, K. Kajimura, and T. Ishiguro, J. Phys. Soc. Jpn. **50**, 3529 (1981).

[68] Y. Maeno, H. Hashimoto, K. Yoshida, S. Nishizaki, T. Fujita, J. G. Bednorz, and F. Lichtenberg, Nature (London) **372**, 532 (1994).

[69] E. Goldobin, M. Yu. Kupriyanov, I. P. Nevirkovets, A. V. Ustinov, M. G. Blamire, and J. E. Evetts, Phys. Rev. B **58**, 15 078 (1998).

[70] S. J. Turneaure, T. R. Lemberger, and J. M. Graybeal, Phys. Rev. Lett. **84**, 987 (2000).

[71] C. C. Homes, T. Timusk, R. Liang, D. A. Bonn, and W. N. Hardy, Phys. Rev. Lett. **71**, 1645 (1993).

[72] J. E. Hirsch, Physica C **199**, 305 (1992); Phys. Rev. B **62**, 14 498 (2000); M. R. Norman, M. Randeria, B. Janko, and J. C. Campuzano, *ibid.* **61**, 14 742 (2000); L. B. Ioffe and A. J. Millis, *ibid.* **61**, 9077 (2000); S. Chakravarty, Eur. Phys. J. B **5**, 337 (1998).